NASA/TP-2017-219597

Neutron Angular Scatter Effects in 3DHZETRN: Quasi-Elastic

John W. Wilson
Old Dominion University, Norfolk, Virginia

Charles M. Werneth, Tony C. Slaba
Langley Research Center, Hampton, Virginia

Francis F. Badavi
Old Dominion University, Norfolk, Virginia

Brandon D. Reddell
Johnson Space Center, Houston, TX

Amir A. Bahadori
Kansas State University, Manhattan, KS

March 2017

NASA STI Program . . . in Profile

Since its founding, NASA has been dedicated to the advancement of aeronautics and space science. The NASA scientific and technical information (STI) program plays a key part in helping NASA maintain this important role.

The NASA STI program operates under the auspices of the Agency Chief Information Officer. It collects, organizes, provides for archiving, and disseminates NASA's STI. The NASA STI program provides access to the NTRS Registered and its public interface, the NASA Technical Reports Server, thus providing one of the largest collections of aeronautical and space science STI in the world. Results are published in both non-NASA channels and by NASA in the NASA STI Report Series, which includes the following report types:

- TECHNICAL PUBLICATION. Reports of completed research or a major significant phase of research that present the results of NASA Programs and include extensive data or theoretical analysis. Includes compilations of significant scientific and technical data and information deemed to be of continuing reference value. NASA counter-part of peer-reviewed formal professional papers but has less stringent limitations on manuscript length and extent of graphic presentations.

- TECHNICAL MEMORANDUM. Scientific and technical findings that are preliminary or of specialized interest, e.g., quick release reports, working papers, and bibliographies that contain minimal annotation. Does not contain extensive analysis.

- CONTRACTOR REPORT. Scientific and technical findings by NASA-sponsored contractors and grantees.

- CONFERENCE PUBLICATION. Collected papers from scientific and technical conferences, symposia, seminars, or other meetings sponsored or co-sponsored by NASA.

- SPECIAL PUBLICATION. Scientific, technical, or historical information from NASA programs, projects, and missions, often concerned with subjects having substantial public interest.

- TECHNICAL TRANSLATION. English-language translations of foreign scientific and technical material pertinent to NASA's mission.

Specialized services also include organizing and publishing research results, distributing specialized research announcements and feeds, providing information desk and personal search support, and enabling data exchange services.

For more information about the NASA STI program, see the following:

- Access the NASA STI program home page at http://www.sti.nasa.gov

- E-mail your question to help@sti.nasa.gov

- Phone the NASA STI Information Desk at 757-864-9658

- Write to:
  NASA STI Information Desk
  Mail Stop 148
  NASA Langley Research Center
  Hampton, VA 23681-2199

NASA/TP-2017-219597

Neutron Angular Scatter Effects in 3DHZETRN: Quasi-Elastic

John W. Wilson
Old Dominion University, Norfolk, Virginia

Charles M. Werneth, Tony C. Slaba
Langley Research Center, Hampton, Virginia

Francis F. Badavi
Old Dominion University, Norfolk, Virginia

Brandon D. Reddell
Johnson Space Center, Houston, TX

Amir A. Bahadori
Kansas State University, Manhattan, KS

National Aeronautics and
Space Administration

Langley Research Center
Hampton, Virginia 23681-2199

March 2017

Available from:

NASA STI Program / Mail Stop 148
NASA Langley Research Center
Hampton, VA 23681-2199
Fax: 757-864-6500

Contents

Figures

Tables

Abstract

The current 3DHZETRN code has a detailed three dimensional (3D) treatment of neutron transport based on a forward/isotropic assumption and has been compared to Monte Carlo (MC) simulation codes in various geometries. In most cases, it has been found that 3DHZETRN agrees with the MC codes to the extent they agree with each other. However, a recent study of neutron leakage from finite geometries revealed that further improvements to the 3DHZETRN formalism are needed. In the present report, angular scattering corrections to the neutron fluence are provided in an attempt to improve fluence estimates from a uniform sphere. It is found that further developments in the nuclear production models are required to fully evaluate the impact of transport model updates. A model for the quasi-elastic neutron production spectra is therefore developed and implemented into 3DHZETRN.

Introduction

The approach taken throughout the development of the HZETRN radiation transport code has been to develop a progression of transport solutions from the simple to increasingly complex, allowing early implementation of high-performance computational procedures based on marching algorithms [Wilson 1977; Wilson et al. 1986a, 1991, 1994; Slaba et al. 2010a] and establishing a converging sequence of approximations with well-defined accuracy criteria. In support of this paradigm, a preliminary nuclear database was established in the early development efforts (circa 1973), so that numerical solutions of the Boltzmann equation could be investigated and developed. This early work is recounted in Wilson et al. [1988a,b; 1991]. The preliminary nuclear database used for numerical transport solution studies proved to be reasonably adequate for application to space system design in the sense that uncertainty was mainly associated with transport solution procedures rather than the nuclear database. Notably, the nucleon portion of the database as described by Wilson et al. [1991] has remained in the HZETRN code (and carried into 3DHZETRN) without any updates. Verification and validation processes of the nuclear and transport models were accomplished over the last several decades using realistic model solutions, convergence criteria, Monte Carlo (MC) simulation, laboratory experiments, and flight data [Wilson et al. 1991, 2005, 2007; Slaba et al. 2013; Matthiä 2016]. Reviews of this development process, including enhanced three dimensional (3D) neutron transport, is given by Wilson et al. [2014a-c, 2015a-c].

Limitations of the current 3DHZETRN code and nuclear database were revealed in part by a study of neutron leakage in finite objects [Wilson et al. 2015b,c] wherein differences in leakage from cube and sphere geometries are obscured by the forward/isotropic (*for*/*iso*) approximation used in 3DHZETRN [Wilson et al. 2014a,b]. Although 3DHZETRN and various MC codes are still plagued by uncertainty in nuclear models and data [Wilson 2014a-c, 2015a], the next step in code development appears as much limited by nuclear model uncertainty as by the transport methods. Therefore, specific problems identified in the neutron leakage study [Wilson et al. 2015b,c] are targeted herein, and some nuclear model improvements are initiated.

In the present report, the *for*/*iso* approximation in 3DHZETRN is replaced by a quasi-elastic/multiple-production (*qe/mp*) separation that allows angular dependence in the neutron production to be easily carried into existing transport procedures. Only minor modifications to the transport formalism and numerical methods are required to implement the *qe/mp* model. It is found that the quasi-elastic component of the neutron production cross section carried over from the preliminary nuclear model of Wilson et al. [1991] is inadequate for this application, and a more detailed model for quasi-elastic nucleon production is considered as a replacement. The new quasi-elastic model is described and implemented into 3DHZETRN transport procedures, and it is shown that modest improvements in the neutron fluence estimates for spherical geometry test-cases are achieved.

Deterministic Code Development

The relevant transport equations are the coupled linear Boltzmann equations derived on the basis of conservation principles [Wilson 1977; Wilson et al. 1991, 2005] for the differential flux (or fluence) density $\phi_j(\boldsymbol{x},\boldsymbol{\Omega},E)$ of a j type particle in the continuous slowing down approximation (CSDA) in which atomic processes are described by the stopping power $S_j(E)$ for each ion type j (vanishes for neutrons $j = n$) as

$$\left[\boldsymbol{\Omega}\bullet\nabla-\frac{1}{A_j}\frac{\partial}{\partial E}S_j(E)+\sigma_j(E)\right]\phi_j(\boldsymbol{x},\boldsymbol{\Omega},E)=\sum_k\int_E^\infty\int_{4\pi}\sigma_{jk}(E,E',\boldsymbol{\Omega},\boldsymbol{\Omega}')\phi_k(\boldsymbol{x},\boldsymbol{\Omega}',E')\,d\boldsymbol{\Omega}'\,dE'\,, \quad (1)$$

and solved subject to a boundary condition over the enclosure of the solution domain. In equation (1), $\sigma_j(E)$ is the total macroscopic cross section for a type j particle with kinetic energy E, and $\sigma_{jk}(E,E',\boldsymbol{\Omega},\boldsymbol{\Omega}')$ is the double differential macroscopic production cross section for nuclear interactions in which a type k particle with kinetic energy E' and direction $\boldsymbol{\Omega}'$ produces a type j particle with kinetic energy E and direction $\boldsymbol{\Omega}$.

The double differential cross sections in equation (1) may be generally separated into reactive (*r*) and elastic (*el*) components according to

$$\sigma_{jk}(E,E',\boldsymbol{\Omega},\boldsymbol{\Omega}')=\sigma_{jk}^{(r)}(E,E',\boldsymbol{\Omega},\boldsymbol{\Omega}')+\sigma_{jk}^{(el)}(E,E',\boldsymbol{\Omega},\boldsymbol{\Omega}')\,. \quad (2)$$

In equation (2), the elastic component is null except for $k = j$ and describes a nuclear collision in which the projectile scatters from the target, but neither the projectile nor target break apart or become excited as a result of the interaction. The reactive component includes all other non-elastic nuclear processes including projectile and target fragmentation, de-excitation, and evaporation. The total cross section in equation (1), $\sigma_j(E)$, may also be separated into elastic and reactive components as in equation (2).

For transport code development efforts leading to 3DHZETRN, the reactive component of the differential cross sections for neutron production ($j = n$) was further separated as [Wilson et al. 2014a,b]

$$\sigma_{nk}^{(r)}(E,E',\boldsymbol{\Omega},\boldsymbol{\Omega}')=\sigma_{nk,for}^{(r)}(E,E',\boldsymbol{\Omega},\boldsymbol{\Omega}')+\frac{1}{4\pi}\sigma_{nk,iso}^{(r)}(E,E')\,. \quad (3)$$

The forward component of the cross section (*for*) is associated mainly with higher energy processes and projectile-like secondaries and is peaked near the projectile energy, E', and direction, $\boldsymbol{\Omega}'$. The isotropic component (*iso*) is mainly associated with lower energy particles produced, including evaporation products, but extends up to moderately high energies. Separation of the cross section into forward and isotropic components was carried out using the Ranft angular factor [Ranft 1980] and will be described later in this report.

An alternative, but related, separation of the reactive cross section for neutron production is given as [Wilson et al. 1988a, 1991]

$$\sigma_{nk}^{(r)}(E,E',\boldsymbol{\Omega},\boldsymbol{\Omega}')=\sigma_{nk,qe}^{(r)}(E,E',\boldsymbol{\Omega},\boldsymbol{\Omega}')+\sigma_{nk,mp}^{(r)}(E,E',\boldsymbol{\Omega},\boldsymbol{\Omega}')\,. \quad (4)$$

In equation (4), the quasi-elastic term (*qe*) represents the spectrum of scattered particles having originated from the projectile and suffering at least one intra-nuclear collision with a nucleon within the target. Charge exchange processes are included in the quasi-elastic term. The multiple-production term (*mp*) accounts for those escaping nucleons and other light ions resulting from intra-nuclear collisions of the quasi-elastic scattered primary particles with nuclear matter and are associated with lower-energy particles produced including target fragments.

Although similar in form, equations (3) and (4) bear important distinctions. Equation (3) provides a convenient separation of phase space into a high energy forward directed component and a lower energy isotropic component. The separation is achieved by identifying backward production represented in the Ranft angular factor as half of the isotropic spectrum. Subtraction and further manipulation then allows the forward component to be deduced [Wilson et al. 2014a,b]. Details of the physical processes included in the forward and isotropic components are not explicitly identified but are assumed to be reasonably characterized within the Ranft angular separation.

Conversely, equation (4) is a more fundamentally physics-based separation of the cross section where specific physical processes and models may be assigned to the quasi-elastic and multiple-production components. One immediate advantage of equation (4) is that angular dependence in the lower energy multiple-production term can be maintained and carried into transport procedures. This work is focused on extending 3DHZETRN to utilize equation (4) instead of equation (3), thereby enabling a more detailed description of angular factors for secondary neutrons. Related efforts are then carried out to improve upon the quasi-elastic component of equation (4).

In past versions of HZETRN and the current version of 3DHZETRN, the quasi-elastic component of equation (4) for nucleons is represented with the parametric form [Wilson et al. 1988b]

$$\sigma^{(r)}_{jk,qe}(E,E',\mathbf{\Omega},\mathbf{\Omega}') = g_R(\theta,E,A_T)\sigma^{(re)}_k(E')\frac{N_{jk,qe}(E')}{C_N E'\left[1+e^{-20(1-E/E')}\right]}, \\ \equiv g_R(\theta,E,A_T)\sigma^{(r)}_{jk,qe}(E,E') \tag{5}$$

where $C_N = 1 - \ln(2) / 20$ is a normalization constant, $N_{jk,qe}(E')$ is the quasi-elastic multiplicity (i.e. average number of type *j* particles produced as a result of a quasi-elastic interaction) [Wilson et al. 1991], and $\sigma^{(re)}_k(E')$ is the reactive component of the total cross section appearing on the left hand side of equation (1). The Ranft angular factor is given by [Ranft 1980]

$$g_R(\theta,E,A_T) = \begin{cases} N_R \exp(-\theta^2 \,/\, \lambda_R) & , \, 0 \le \theta \le \pi \,/\, 2 \\ N_R \exp(-\pi^2 \,/\, 4\lambda_R) & , \, \pi \,/\, 2 < \theta \le \pi \end{cases}, \tag{6}$$

where N_R is an energy dependent normalization factor defined such that $\int g_R(\theta,E,A_T)d\mathbf{\Omega} = 1$ and cos θ = $\mathbf{\Omega}$·$\mathbf{\Omega}'$. The Ranft width factor is

$$\lambda_R = (0.12 + 0.00036A_T) \,/\, E\,, \tag{7}$$

where A_T is the mass of the struck nucleus.

The multiple-production term in equation (4) represents highly spectrally dispersed particles of lower energy including the de-excitation spectrum [Wilson and Costner 1977, Wilson et al. 1988b] with spectral components given by

$$\sigma^{(r)}_{jk,mp}(E,E',\mathbf{\Omega},\mathbf{\Omega}') = g_R(\theta,E,A_T)\sigma^{(r)}_k(E')\sum_{i=1}^{3} N^{(i)}_{jk,mp}(E')\frac{e^{-E/\alpha_i}}{\alpha_i\left[1-e^{-E'/\alpha_i}\right]}, \\ = g_R(\theta,E,A_T)\sigma^{(r)}_{jk,mp}(E,E') \tag{8}$$

where $N^{(i)}_{jk,mp}(E')$ are multiplicities from the Bertini model, and α_i are shape parameters as described by Wilson et al. [1991].

As discussed previously in this section, early development efforts of 3DHZETRN [Wilson et al. 2014a-c, 2015a], utilized the *for*/*iso* approximation to provide a convenient separation of phase space. Although not obvious in equations (3) - (8), the isotropic component of the cross section extends up to relatively high fragment energies and may include various physical processes with pronounced angular dependence. To illustrate this point, Fig. 1 shows the forward and isotropic neutron production fractions for protons and neutrons incident on aluminum. The isotropic fraction is defined as

$$F_{iso}(E') = \frac{2\int_0^\infty \int_{2\pi B} \sigma^{(r)}_{jk}(E,E',\mathbf{\Omega},\mathbf{\Omega}')\,dE\,d\mathbf{\Omega}}{\int_0^\infty \int_{4\pi} \sigma^{(r)}_{jk}(E,E',\mathbf{\Omega},\mathbf{\Omega}')\,dE\,d\mathbf{\Omega}}, \tag{9}$$

where the integral in the numerator is only taken over the back hemisphere, $2\pi B$, and then doubled to represent the isotropic component of the cross section as defined by Wilson et al. [2014a-c, 2015a]. The forward component is simply one minus the isotropic component given in equation (9). Although the isotropic component dominates for projectile energies below ~20 MeV, as would be expected, it accounts for more than half of the cross section for projectile energies in the GeV region. Certainly, portions of the fragment spectrum for such high energy projectiles will include angular dependence that is not captured by the *for*/*iso* approximation.

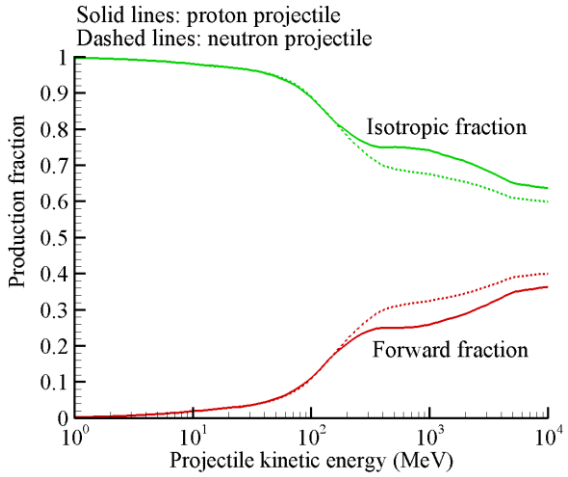

Fig. 1. Isotropic and forward fraction of neutrons produced in nuclear reactions by nucleons incident on aluminum according to the current HZETRN database.

A brief description of the elastic cross section is given here; although, no modifications to the transport or nuclear model for elastic interactions are considered in this work. The elastic scattering components are found using the differential angle distribution of Wilson et al. [1991] consisting of an *S*-wave amplitude and Chew's impulse approximation [Chew 1951] representing the higher order angular dispersion [Wilson et al. 1991] (similar to the approach of Wilson [1973] for the three nucleon problem). A linear energy factor is applied to the *S*-wave cross section to match the neutron KERMA as described in Wilson et al. [1991]. For further comparison, the fraction of *S*-wave scattering according to this model has been evaluated and compared with the Evaluated Nuclear Data File [ENDF 2016] derived *S*-wave fraction as shown in Fig. 2. It is clear that this simple scheme provides a reasonable first order approximation to the nuclear elastic scattering.

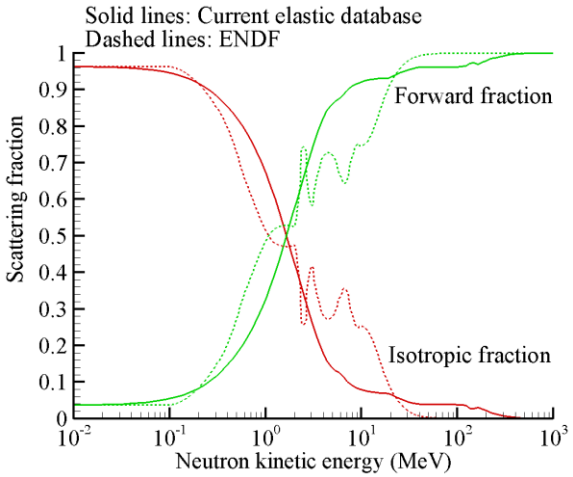

Fig. 2. Isotropic scattering and forward scattering fractions of neutrons in aluminum according to the current elastic database and ENDF database.

Transport Model Development: Historical

A prime limitation in developing solutions for equation (1) lies in evaluating the integral over $d\mathbf{\Omega}'$ at any arbitrary location within the media. The approach to a practical solution of equation (1) is to develop a progression

of solution methods from the simple to increasingly complex allowing early implementation of high-performance computational procedures and establishing a converging sequence of approximations with well-defined accuracy criteria and means of verification and validation. The first step, leading to the lowest order solution, simplifies the evaluation over $d\boldsymbol{\Omega}'$ by introducing the straight-ahead approximation as guided by the nucleon transport studies of Alsmiller et al. [1965]. In these studies, MC methods were utilized, and the differential cross sections were approximated as

$$\sigma_{jk}(E,E',\boldsymbol{\Omega},\boldsymbol{\Omega}') = \sigma_{jk}(E,E')\delta(\boldsymbol{\Omega}-\boldsymbol{\Omega}')\,, \tag{10}$$

resulting in dose and dose equivalent per unit fluence to be within the statistical uncertainty of the MC result obtained using the fully angle dependent cross sections in slab geometry [Alsmiller et al. 1965, Wilson et al. 1991, 2014a-c, 2015a]. Using asymptotic expansions about angular divergence parameters, it has been demonstrated that the error in using equation (10) for solving equation (1) is on the order of the square of the ratio of distance of divergence (few centimeters) to radius of curvature of the shield (few to several m) resulting in a small relative error in most human rated space systems [Wilson and Khandelwal 1974, Wilson et al. 1991]. The straight-ahead approximation of equation (10) formed the basis of the early versions of HZETRN and related numerical marching algorithms, for which the verification and validation processes are described elsewhere [Wilson et al. 2005, 2006, 2014a-c, 2015a].

In the early Boltzmann transport studies of Wilson and Lamkin [1974, 1975] and Lamkin [1974], it was demonstrated that after neutrons are produced by a proton beam, the recoupling of neutrons back to the proton field is limited, but the neutron fields tend to build-up with increasing penetration depth. This mainly occurs since many protons produced by neutron-induced interactions are of lower energy and are quickly removed by atomic interactions (especially the isotropically produced protons). The probability of even a 100 MeV proton to undergo a nuclear reaction is only several percent [Wilson et al. 1991, 2005]. The low-energy neutrons on the other hand have no effective atomic interactions and propagate until a nuclear interaction occurs or they escape through the media boundary. Yet, the low-energy protons and other light ions produced in tissue through neutron collisions contribute significantly to biological injury and must be accounted for in transport methods [Foelsche et al. 1974]. This was the basis of the studies of Heinbockel and co-workers [2003] starting with Clowdsley et al. [2000, 2001] using the NUCFRG2 database [Wilson et al. 1987a,b; 1995; 1998].

Accordingly, improved methods for solving the neutron component of equation (1) were developed [Heinbockel et al. 2003; Slaba et al. 2010b]. These solutions approximated the neutron double differential cross sections as the sum of forward (*f*) and backward (*b*) components according to

$$\sigma_{nk}(E,E',\boldsymbol{\Omega},\boldsymbol{\Omega}') = \sigma_{nk,f}(E,E',\boldsymbol{\Omega},\boldsymbol{\Omega}') + \sigma_{nk,b}(E,E',\boldsymbol{\Omega},\boldsymbol{\Omega}')\,. \tag{11}$$

Implementation of equation (11) resulted in the bi-directional code in common use for spacecraft design. A similar bi-directional approximation for the light ions was considered by Cucinotta et al. [1990] and Shavers et al. [1996] to study interface transition effects but was not integrated into the HZETRN software.

Transport Model Development: Forward/Isotropic

A sequence of approximations that span the formalisms from the simple straight-ahead and bi-directional methods to more complex propagation algorithms has been developed and is based on a simple *for*/*iso* assumption given previously by equation (3). The isotropic component is associated with lower-energy neutrons produced and defined by

$$\sigma^{(r)}_{nk,iso}(E,E') = 2\int_{2\pi B}\sigma^{(r)}_{nk}(E,E',\boldsymbol{\Omega},\boldsymbol{\Omega}')\,d\boldsymbol{\Omega}\,, \tag{12}$$

where $2\pi B$ represents the backward hemisphere. The forward component,

$$\sigma^{(r)}_{nk,for}(E,E',\boldsymbol{\Omega},\boldsymbol{\Omega}') = \sigma^{(r)}_{nk}(E,E',\boldsymbol{\Omega},\boldsymbol{\Omega}') - \frac{1}{4\pi}\sigma^{(r)}_{nk,iso}(E,E')\,, \tag{13}$$

is associated mainly with direct quasi-elastic events [Wilson 1977, Wilson et al. 1988b], although other processes are included, and is highly peaked in the forward direction.

The governing transport equation within the CSDA, ignoring multiple Coulomb scattering, is given by equation (1), and the total cross sections and double differential cross sections are the nuclear scattering and reaction values. The double differential cross sections are represented by equations (2) and (3). With the demonstrated success of the bi-directional approximation [Slaba et al. 2010b; Heinbockel et al. 2011; Wilson et al. 2014a-c, 2015a] for neutron fields, the solution $\phi_j(\boldsymbol{x},\boldsymbol{\Omega},E)$ is divided into forward and isotropic components and the forward component is assumed to satisfy

$$\left[\boldsymbol{\Omega}\bullet\nabla-\frac{1}{A_j}\frac{\partial}{\partial E}S_j(E)+\sigma_j(E)\right]\phi_{j,for}(\boldsymbol{x},\boldsymbol{\Omega},E)=\sum_k\int_E^\infty\sigma_{jk,for}(E,E')\phi_{k,for}(\boldsymbol{x},\boldsymbol{\Omega},E')\,dE', \tag{14}$$

where the forward component of the cross section is given as

$$\sigma_{jk,for}(E,E')=\begin{cases}\displaystyle\int_{4\pi}\sigma_{jk}(E,E',\boldsymbol{\Omega},\boldsymbol{\Omega}')\,d\boldsymbol{\Omega} & ,\ j\neq n\\ \displaystyle\int_{4\pi}\sigma^{(r)}_{jk,for}(E,E',\boldsymbol{\Omega},\boldsymbol{\Omega}')+\sigma^{(el)}_{jk}(E,E',\boldsymbol{\Omega},\boldsymbol{\Omega}')\,d\boldsymbol{\Omega} & ,\ j=n\end{cases}, \tag{15}$$

and the straight-ahead approximation is used to represent the angular spectra of equation (15). Note that $\boldsymbol{\Omega}$ only appears as a parameter in equation (14) and can be evaluated according to the boundary condition that is set as the incident fluence from direction $\boldsymbol{\Omega}_0$ at the boundary as shown in Fig. 3.

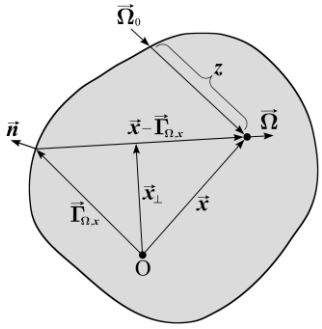

Fig. 3. Geometry for 3D transport procedure.

The isotropic component of the neutron field is obtained by solving

$$\begin{aligned}[\boldsymbol{\Omega}\bullet\nabla+\sigma_n(E)]\phi_{n,iso}(\boldsymbol{x},\boldsymbol{\Omega},E)=&\int_E^\infty\int_{4\pi}\sigma_{nn}(E,E',\boldsymbol{\Omega},\boldsymbol{\Omega}')\phi_{n,iso}(\boldsymbol{x},\boldsymbol{\Omega}',E')\,d\boldsymbol{\Omega}'\,dE'\\&+\sum_k\int_E^\infty\sigma^{(r)}_{nk,iso}(E,E')\phi_{k,for}(\boldsymbol{x},\boldsymbol{\Omega}_0,E')\,dE'\end{aligned} \tag{16}$$

using a bi-directional approximation along $\boldsymbol{\Omega}$ [Wilson et al. 2014a-c, 2015a-c]. Coupling between the forward solution of equation (14) and the isotropic neutron field is expressed through the perturbation given by the last term on the right hand side of equation (16). Although $\phi_{n,iso}(\boldsymbol{x},\boldsymbol{\Omega},E)$ is generated by the isotropic cross section term, the resulting fluence is not necessarily isotropic. A final step in the solution methodology is to compute the source of light ions produced from the lower energy isotropic neutrons. Once this source is computed, the isotropic component of the light ion flux is solved under the assumption that no further nuclear collisions occur, giving partial 3D treatment to low energy charged particles.

The solution of these coupled equations (14) and (16) and some of their limitations are thoroughly discussed by Wilson et al. [2014a-c, 2015a-c]. The resulting transport algorithm allows direct evaluation of the straight-ahead and bi-directional approximation error at least in the context of the *for*/*iso* interaction approximation.

Although the *for*/*iso* formalism has yielded improved solutions over the straight-ahead and bi-directional models, limitations have also been discussed in previous sections and noted in recent work [Wilson et al. 2015b,c, Slaba et al. 2016] that will be addressed herein. The approach will be a more direct solution to equation (1) using an improved representation of neutron cross sections as in equations (4) - (7).

Transport Model Development: Quasi-Elastic/Multiple-Production

As a further refinement of detail for 3DHZETRN, equation (4) is now utilized to separate the reaction cross section for neutron production. In this more detailed approach, the fluence is separated into a high energy forward (*hef*) and angular (*ang*) component as

$$\phi_j(\boldsymbol{x},\boldsymbol{\Omega},E) = \phi_{j,hef}(\boldsymbol{x},\boldsymbol{\Omega},E) + \phi_{j,ang}(\boldsymbol{x},\boldsymbol{\Omega},E)\,. \tag{17}$$

Equations (4) and (17) are substituted into equation (1), and the *hef* fluence is defined to satisfy

$$\left[\boldsymbol{\Omega}\bullet\nabla - \frac{1}{A_j}\frac{\partial}{\partial E}S_j(E) + \sigma_j(E)\right]\phi_{j,hef}(\boldsymbol{x},\boldsymbol{\Omega},E) = \sum_k \int_E^\infty \tilde{\sigma}_{jk}(E,E')\phi_{k,hef}(\boldsymbol{x},\boldsymbol{\Omega},E')\,dE'\,, \tag{18}$$

where the cross section on the right hand side of equation (18) is written as

$$\tilde{\sigma}_{jk}(E,E') = \begin{cases} \displaystyle\int_{4\pi}\sigma_{jk}(E,E',\boldsymbol{\Omega},\boldsymbol{\Omega}')\,d\boldsymbol{\Omega} & ,\ j \neq n \\ \displaystyle\int_{4\pi}\sigma^{(r)}_{jk,qe}(E,E',\boldsymbol{\Omega},\boldsymbol{\Omega}') + \sigma^{(el)}_{jk}(E,E',\boldsymbol{\Omega},\boldsymbol{\Omega}')\,d\boldsymbol{\Omega} & ,\ j = n \end{cases}. \tag{19}$$

The angular spectra in equation (19) are represented within the straight-ahead approximation. The equation for the angular component of the neutron field is

$$\begin{aligned}[\boldsymbol{\Omega}\bullet\nabla + \sigma_n(E)]\phi_{n,ang}(\boldsymbol{x},\boldsymbol{\Omega},E) = &\int_E^\infty\int_{4\pi}\sigma_{nn}(E,E',\boldsymbol{\Omega},\boldsymbol{\Omega}')\phi_{n,ang}(\boldsymbol{x},\boldsymbol{\Omega}',E')\,d\boldsymbol{\Omega}'\,dE' \\ &+\sum_k\int_E^\infty\sigma^{(r)}_{nk,mp}(E,E',\boldsymbol{\Omega},\boldsymbol{\Omega}_0)\phi_{k,hef}(\boldsymbol{x},\boldsymbol{\Omega}_0,E')\,dE'\end{aligned}\,. \tag{20}$$

Note that $\phi_{n,ang}(\boldsymbol{x},\boldsymbol{\Omega},E)$ is generated by the angular dependent multiple-production interaction term, $\sigma_{nk,mp}(E,E',\boldsymbol{\Omega},\boldsymbol{\Omega}_0)$, and is not isotropic.

The coupled equations (18) and (20) appear similar to equations (14) and (16) of the *for*/*iso* model with the exception that the cross section in the coupling source term is no longer isotropic. Despite this added complexity, equations (18) and (20) can be solved using the exact same numerical solution methodologies used in the *for*/*iso* model but with a modified source term. This will allow a direct evaluation of the errors associated with the previous *for*/*iso* formalism.

Equation (20) is solved by representing the double differential cross section of equation (20) within the bi-directional approximation, given by

$$\sigma_{nn}(E,E',\boldsymbol{\Omega},\boldsymbol{\Omega}') = \sigma_{nn,f}(E,E')\delta(\boldsymbol{\Omega}-\boldsymbol{\Omega}') + \sigma_{nn,b}(E,E')\delta(\boldsymbol{\Omega}+\boldsymbol{\Omega}')\,, \tag{21}$$

$$\sigma_{nn,f}(E,E') = \int_{2\pi F}\sigma_{nn}(E,E',\boldsymbol{\Omega},\boldsymbol{\Omega}')d\boldsymbol{\Omega} = \sigma^{(r)}_{nn,qe}(E,E') + \sigma^{(r)}_{nn,mp(f)}(E,E') + \sigma^{(el)}_{nn,(f)}(E,E')\,, \tag{22}$$

and

$$\sigma_{nn,b}(E,E') = \int_{2\pi B}\sigma_{nn}(E,E',\boldsymbol{\Omega},\boldsymbol{\Omega}')d\boldsymbol{\Omega} = \sigma^{(r)}_{nn,mp(b)}(E,E') + \sigma^{(el)}_{nn,(b)}(E,E')\,, \tag{23}$$

where the forward (*f*) and backward (*b*) components of the multiple-production cross section are computed as

$$\sigma^{(r)}_{nn,mp(f)}(E,E') = \int_{2\pi F} \sigma^{(r)}_{nn,mp}(E,E',\boldsymbol{\Omega},\boldsymbol{\Omega}')d\boldsymbol{\Omega}\,, \tag{24}$$

$$\sigma^{(r)}_{nn,mp(b)}(E,E') = \int_{2\pi B} \sigma^{(r)}_{nn,mp}(E,E',\boldsymbol{\Omega},\boldsymbol{\Omega}')d\boldsymbol{\Omega}\,. \tag{25}$$

In equations (22) - (25), $2\pi F$ and $2\pi B$ represent integration over the forward and backward hemispheres relative to $\boldsymbol{\Omega}'$. The subscripts (*f*) and (*b*) refer to the forward hemispheric and backward hemispheric components of the multiple-production neutron cross section, respectively. The forward and backward components of the elastic cross sections appearing in equations (22) and (23) are similarly evaluated by integrating the elastic values over the forward and backward hemispheres.

Using equations (21) - (23) in equation (20) results in a coupled set of equations for $\phi_{n,ang}(\boldsymbol{x},\boldsymbol{\Omega},E)$ and $\phi_{n,ang}(\boldsymbol{x},-\boldsymbol{\Omega},E)$. The equation for $\phi_{n,ang}(\boldsymbol{x},\boldsymbol{\Omega},E)$ is given by

$$\begin{aligned}[\boldsymbol{\Omega}\bullet\nabla+\sigma_n(E)]\phi_{n,ang}(\boldsymbol{x},\boldsymbol{\Omega},E) = &\int_E^\infty \sigma_{nn,f}(E,E')\phi_{n,ang}(\boldsymbol{x},\boldsymbol{\Omega},E')\,dE' \\ &+\int_E^\infty \sigma_{nn,b}(E,E')\phi_{n,ang}(\boldsymbol{x},-\boldsymbol{\Omega},E')\,dE' \\ &+\sum_k \int_E^\infty \sigma^{(r)}_{nk,mp}(E,E',\boldsymbol{\Omega},\boldsymbol{\Omega}_0)\phi_{k,hef}(\boldsymbol{x},\boldsymbol{\Omega}_0,E')\,dE'\end{aligned}\,. \tag{26}$$

The equation for $\phi_{n,ang}(\boldsymbol{x},-\boldsymbol{\Omega},E)$ is

$$\begin{aligned}[-\boldsymbol{\Omega}\bullet\nabla+\sigma_n(E)]\phi_{n,ang}(\boldsymbol{x},-\boldsymbol{\Omega},E) = &\int_E^\infty \sigma_{nn,f}(E,E')\phi_{n,ang}(\boldsymbol{x},-\boldsymbol{\Omega},E')\,dE' \\ &+\int_E^\infty \sigma_{nn,b}(E,E')\phi_{n,ang}(\boldsymbol{x},\boldsymbol{\Omega},E')\,dE' \\ &+\sum_k \int_E^\infty \sigma^{(r)}_{nk,mp}(E,E',-\boldsymbol{\Omega},\boldsymbol{\Omega}_0)\phi_{k,hef}(\boldsymbol{x},\boldsymbol{\Omega}_0,E')\,dE'\end{aligned}\,. \tag{27}$$

The second integral appearing on the right hand side of equations (26) and (27) is the coupling term between the $\boldsymbol{\Omega}$ and $-\boldsymbol{\Omega}$ multiple-production components. Equations (26) and (27) represent a coupled set of partial differential equations that are solved efficiently using a Neumann series approach as shown by Slaba et al. [2010b]. This series is expected to converge quickly since $\sigma_{nn,f} \gg \sigma_{nn,b}$ is required to conserve momentum.

Similar to the *for/iso* formalism, a final step in the solution methodology is to compute the source of light ions produced from the neutrons of equations (26) and (27). Once this source is computed, the multiple-production component of the light ion flux is solved under the assumption that no further nuclear collisions occur, giving partial 3D treatment to these charged particles.

Simple Homogenous Spherical Geometry

Simple geometry and source orientation are chosen to allow efficient MC simulation for comparison with with the above formalisms [Wilson et al. 2014a,b]. The geometry herein is taken as a simple aluminum sphere with a 40 g/cm^2 diameter. Target points are placed at depths along the *z*–axis. The external radiation environment is assumed to be anti-parallel with the *z*-axis, uniform in the *x*-*y* plane, positioned above the sphere, and directed down onto the top of the sphere as shown in Fig. 4. The February 1956 Solar Particle Event (SPE) spectrum [Webber 1966] is assumed to be incident from above. Along with 3DHZETRN, the MC codes Geant4 [Agostinelli et al. 2003], FLUKA [Fasso et al. 2005, Battistoni et al. 2007] and PHITS [Sato et al. 2013] were evaluated. Further details for the Monte Carlo codes and simulation setup can be found in Wilson et al. [2014a,b].

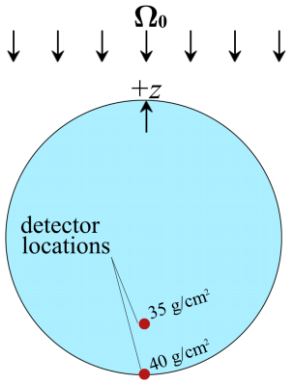

Fig. 4. Spherical geometry and external source orientation for benchmark comparisons.

The solution for N = 18 of both the *for*/*iso* and *qe*/*mp* formalisms are shown in Fig. 5 along with results from the MC simulations. Also shown is the *hef* component of the *qe*/*mp* solution to be compared with the *for* component of the *for/iso* solution. The most notable feature is the greatly increased total neutron fluence in the 10 MeV to few hundred MeV domain in going from the *for*/*iso* approximation to the *qe*/*mp* approximation. The main difference appears to be in the *hef* and *for* components of the fluence.

This difference arises for two reasons. First, the low energy angle distribution by Ranft becomes increasingly isotropic with decreasing fragment energy, and second, the quasi-elastic energy spectrum remains constant over most of its domain even at low energies as shown in Fig. 6 and equation (5). Therefore, the separation of the quasi-elastic component in the straight-ahead approximation is vastly different than the forward component of the *for*/*iso* approximation. The fault in the drop in the neutron fluence near 100 MeV in Fig. 5 results from the application of the *for*/*iso* approximation to the inadequate description of the nuclear induced spectrum, and an improved nuclear model is required. To begin correction of these factors we will develop an alternate and more reliable energy spectral distribution for the quasi-elastic cross section.

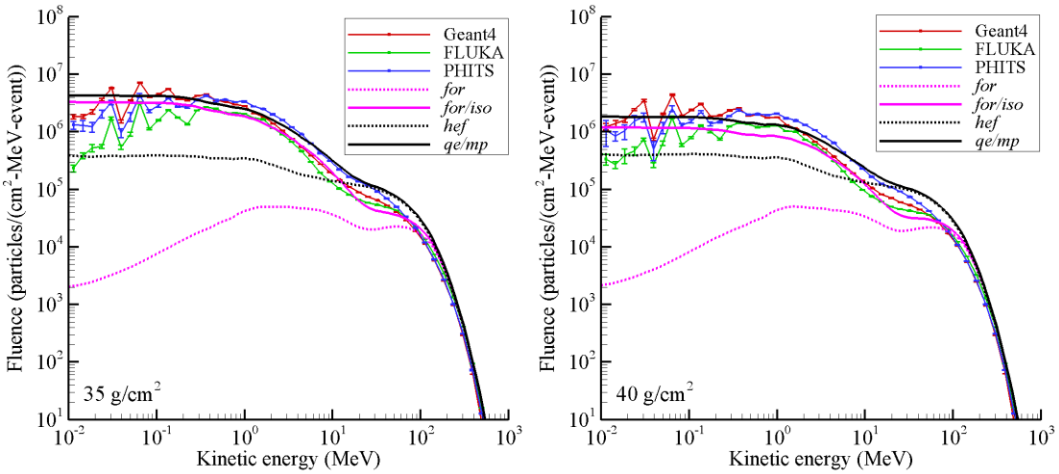

Fig. 5. Neutron fluence spectra at 35 g/cm^2 (left) and 40 g/cm^2 (right) in sphere exposed to Webber SPE. Results from 3DHZETRN (N = 18) using the *for*/*iso* and *qe/mp* models are shown along with MC evaluations.

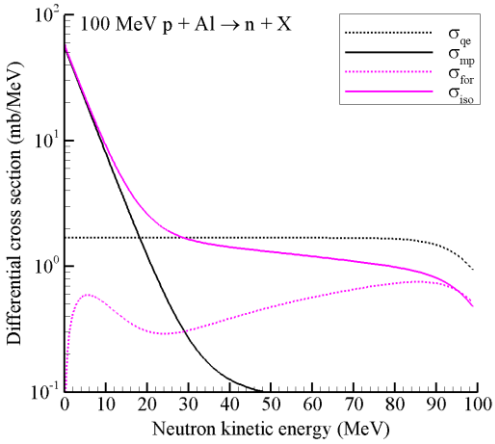

Fig. 6. Neutron production cross sections for 100 MeV proton collisions in the *qe*/*mp* and *for*/*iso* formalisms.

A Dynamical Theory of Quasi-Elastic Scattering

In this section, a new model for estimating the quasi-elastic component of the neutron production cross section is described. Two solution methodologies are formulated to solve the model equations and are shown to give equivalent numerical results. A method for integrating the new quasi-elastic model into 3DHZETRN is also described.

Historical high-energy nuclear reaction theory considered a rapid sequence of binary interactions within nuclear matter followed by a slower de-excitation process and allowed various reaction channels to be estimated [Serber 1947]. Initial implementation efforts of this model were based largely on semi-classical theory using mean free paths in nuclear matter and angular scattering models limited only by the Pauli Exclusion Principle (PEP) in the lowest energy and momentum transfer processes. The modern versions of this development are the intra-nuclear cascade (INC) codes utilizing computer generated random number sequences (initial attempts were two dimensional simulations using random number tables [Goldberger 1948]). Related to the INC model is a Boltzmann equation description, considered in this work, able to produce an analytic formalism equivalent to the INC stochastic results.

The relevant transport equation is the linear Boltzmann equation derived on the basis of conservation principles for the flux density $\phi(z,E)$ (nucleons/(fm^2-MeV)) of nucleons moving through nuclear matter with kinetic energy E (MeV). Within the lowest order one dimensional approximation [Wilson et al. 1986b], the transport equation is

$$\left[\frac{\partial}{\partial z} + \sigma(E)\right]\phi(z,E) = \int \sigma(E,E')\phi(z,E')dE', \tag{28}$$

subject to the boundary condition $\phi(0,E) = \delta(E - E_L)$, with E_L being the lab energy (MeV) of the assumed mono-energetic beam with unit intensity incident on nuclear matter. Within the region of nuclear matter in which the target nucleus is represented, transport processes are modified by a liquid drop model with a potential well depth of V_0 and a Fermi energy of ε_f representing the top level of the Fermi sea below the binding potential, V_b, of the least bound nucleon. Note that the lowest energy transfers, Δ, given by $\Delta < \varepsilon_f - \varepsilon$, are blocked by the PEP and that collisions on the range of $\varepsilon_f - \varepsilon < \Delta < V_0$ contribute to nuclear excitation. The solution domain of equation (28) is approximately over $\{\varepsilon_f, E_L-\varepsilon_f\}$. For present purposes, the nuclear binding potential is ignored, and the integration limits are taken as $\{E, E_L-\varepsilon_f\}$ with ε_f = 24.5 MeV.

In equation (28), $\sigma(E)$ is the inverse mean free path in nuclear matter in units of 1/fm, and $\sigma(E,E')$, in units of 1/(fm-MeV), represents the processes by which a nucleon with energy E' (MeV) collides with nuclear matter, and a nucleon emerges with energy E (MeV). The following parameterization is used in this work for $\sigma(E)$, for E between 40 MeV and 500 MeV [Wilson et al. 1987b]

$$\sigma(E) = E^{0.26} \; / \, 16.6 \, , \tag{29}$$

where the energy dependence is partially a result of PEP effects which reduce the cross section and increase the mean free path for a nucleon within the struck nucleus (especially at low energy), as has been determined empirically [Dymarz and Kohmura 1982]. For energies below 40 MeV and above 500 MeV, equation (29) is evaluated directly as an extrapolation.

The cross section on the right hand side of equation (28), is further discussed in Wilson et al. [1986b, 1991] and approximated herein by

$$\begin{aligned} \sigma(E,E') &= \sigma(E')B(E')\frac{e^{-B(E')(E'-E)}}{1-e^{-B(E')E'}} + \sigma(E')B(E')\frac{e^{-B(E')E}}{1-e^{-B(E')E'}} \, , \\ &\equiv \sigma_0(E,E') + \sigma_1(E,E') \end{aligned} \tag{30}$$

where $B(E')$ is the slope parameter given by [Wilson et al. 1991]

$$B(E') = 2mc^2 10^{-6} \;\; 3.5 + 30e^{-E'/200} \;\; , \tag{31}$$

and mc^2 is the nucleon rest energy (938 MeV). The first term in equation (30), labeled as $\sigma_0(E,E')$, accounts for elastic scattering of an incoming nucleon from a target nucleon and dominates for values of E near the incident energy E'. The second term, labeled as $\sigma_1(E,E')$, provides the spectrum of recoil nucleons dislodged from nuclear matter and dominates for small values of E. In the present formalism, details of nuclear binding effects (including Pauli blocking) and isospin are ignored for simplicity. Such corrections will be treated in a later work, once proof of principle is achieved in the present study.

The operator on the left hand side of equation (28) can be inverted using an integrating factor and written as the Volterra integral equation

$$\phi(z,E) = e^{-\sigma(E)z}\phi(0,E) + \int_0^z \int_E^{E_L} e^{-\sigma(E)(z-z')}\sigma(E,E')\phi(z',E')dE'dz' \, . \tag{32}$$

In order to establish the scattering properties of primary nucleons in nuclear media, solutions for equation (32) will be considered using only the $\sigma_0(E,E')$ component of the cross section in equation (30). It will then be shown in the following sections that such solutions may be used to compute improved quasi-elastic cross sections needed for 3DHZETRN, as discussed in the previous section. Equation (32) may be equivalently solved as a perturbation series [Wilson and Lamkin 1974, 1975; Wilson et al. 1986b] or with marching procedures [Wilson et al. 1988a]. The next two sub-sections describe both solution methodologies, and comparisons are provided as a verification of the numerical implementations.

Note, the use of the term "multiple scattering" herein has a specific meaning and is more limited than that used elsewhere [Wilson 1974, 1975]. In this case, incident nucleons passing through the target may suffer one or more collisions with target nucleons; these multiple collisions are referred to as multiple scattering and are represented in solutions to equation (32) utilizing only the $\sigma_0(E,E')$ component of the interaction cross section. Related to this terminology, the quasi-elastic cross section is defined in the next section in terms of the multiple scattering nucleon fluence transmitted through a specified finite region of nuclear matter.

Perturbative Solution

A perturbative solution methodology for equation (32) is developed in this section and is used to verify more efficient computational procedures based on a marching algorithm. The first term in the perturbative solution is obtained by neglecting the integrals on the right hand side of equation (32) and consists of the un-collided particle beam given as

$$\begin{aligned}\phi_0(z,E) &= e^{-\sigma(E)z}\phi(0,E) \\ &= e^{-\sigma(E)z}\delta(E-E_L) \\ &\equiv \phi_0^{(s)}(z,E)\ .\end{aligned} \tag{33}$$

Higher order terms in the series solution are found by successive iterations of the equation [Wilson and Lamkin 1974, 1975; Wilson et al. 1986a]

$$\phi_i^{(s)}(z,E) = \int_0^z \int_E^{E_L} e^{-\sigma(E)(z-z')}\sigma_0(E,E')\phi_{i-1}^{(s)}(z',E')dE'dz'\,, \tag{34}$$

for $i \geq 1$. The solution for primary nucleons suffering only one collision can be evaluated analytically and is given by

$$\begin{aligned}\phi_1^{(s)}(z,E) &= \int_0^z \int_E^{E_L} e^{-\sigma(E)(z-z')}\sigma_0(E,E')\phi_0^{(s)}(z',E')dE'dz' \\ &= \sigma_0(E,E_L)\frac{e^{-\sigma(E)z} - e^{-\sigma(E_L)z}}{\sigma(E_L)-\sigma(E)}\ .\end{aligned} \tag{35}$$

The next term of the multiple scattering series represents those nucleons suffering two collisions and is given by

$$\begin{aligned}\phi_2^{(s)}(z,E) &= \int_0^z \int_E^{E_L} e^{-\sigma(E)(z-z')}\sigma_0(E,E')\phi_1^{(s)}(z',E')dE'dz' \\ &= \int_E^{E_L} \frac{\sigma_0(E,E')\sigma_0(E',E_L)}{\sigma(E_L)-\sigma(E')}\left[\frac{e^{-\sigma(E_L)z} - e^{-\sigma(E)z}}{\sigma(E_L)-\sigma(E)} - \frac{e^{-\sigma(E')z} - e^{-\sigma(E)z}}{\sigma(E')-\sigma(E)}\right]dE'\ .\end{aligned} \tag{36}$$

The remaining integral in equation (36) is difficult to evaluate analytically but is easily handled with numerical quadrature. The remaining higher order terms are found by evaluating equation (34) numerically.

Note that this is similar to the perturbation series solutions developed many years ago [Wilson and Lamkin 1974, 1975, Lamkin 1974, Wilson et al. 1986b]. In the above, only the fate of incident nucleons is described, and the two nucleonic components {*p*,*n*} have been ignored. However, the formalism can be easily extended to include multiple constituents {*p*,*n*} and charge exchange cross sections (see Wilson et al. [1991]). The complete solution for the scattered primary nucleons that suffer at least one collision in nuclear matter is given as

$$\phi_{ms}(z,E) = \sum_{i=1}^{\infty} \phi_i^{(s)}(z,E)\,, \tag{37}$$

where the subscript *ms* is used to denote the multiple scattering perturbative solution. Note that the $\phi_0^{(s)}(z,E)$ term represents the incident fluence reaching depth *z* without suffering a nuclear elastic scattering event (neglecting the important diffractive components [Wilson 1974, 1975]) and is therefore not part of the multiple scattering solution in equation (37).

Marching procedure

Highly efficient numerical marching procedures have also been developed for equation (28). The solution proceeds by first noting that equation (32) can be equivalently written over a small step-size, *h*, given by

$$\phi(z+h,E) = e^{-\sigma(E)h}\phi(z,E) + \int_0^h \int_E^{E_L} e^{-\sigma(E)(h-t)}\sigma_0(E,E')\phi(z+t,E')dE'dt\,, \tag{38}$$

where only the σ_0 component of the cross section is used, as in the previous section. Equation (38) propagates both the scattered and un-collided primary fluence over a step-size of *h*. However, for comparison to the multiple scattering solution of equation (37), the un-collided primary fluence needs to be removed from the marching procedure. This is achieved by noting that the fluence in equation (38) can be written as

$$\phi(z,E) = \phi_0(z,E) + \phi_{sc}(z,E)\,, \tag{39}$$

where $\phi_0(z,E)$ represents the un-collided primary nucleons as in the previous section, and $\phi_{sc}(z,E)$ represents the nucleons suffering at least one nuclear collision. The solution for the scattered fluence, $\phi_{sc}(z,E)$, may be compared directly to the multiple scattering solution given by equation (37). The terminology (scattered vs. multiple scattering) and notation has been modified here to distinguish between the perturbative method and marching procedure solutions.

If equation (39) is substituted into equation (38), one obtains

$$\begin{aligned}\phi_{sc}(z+h,E) = {} & e^{-\sigma(E)h}\phi_{sc}(z,E) \\ & +\sigma_0(E,E_L)e^{-\sigma(E_L)z}\,\frac{e^{-\sigma(E)h} - e^{-\sigma(E_L)h}}{\sigma(E_L)-\sigma(E)} \\ & +\int_0^h\int_E^{E_L} e^{-\sigma(E)(h-t)}\sigma_0(E,E')\phi_{sc}(z+t,E')dE'\,dt\,,\end{aligned} \tag{40}$$

where equation (33) has been used to relate the un-collided primary nucleon field at an arbitrary depth to the boundary condition. An explicit marching algorithm is derived by noting that [Wilson et al. 1991]

$$\phi_{sc}(z+t,E') = e^{-\sigma(E')t}\phi_{sc}(z,E') + O(t)\,. \tag{41}$$

If equation (41) is substituted into the integrand of equation (40), one obtains

$$\begin{aligned}\phi_{sc}(z+h,E) = {} & e^{-\sigma(E)h}\phi_{sc}(z,E) \\ & +\sigma_0(E,E_L)e^{-\sigma(E_L)z}\,\frac{e^{-\sigma(E)h} - e^{-\sigma(E_L)h}}{\sigma(E_L)-\sigma(E)} \\ & +\int_0^h\int_E^{E_L} e^{-\sigma(E)(h-t)}e^{-\sigma(E')t}\sigma_0(E,E')\phi_{sc}(z,E')dE'\,dt + O(h^2).\end{aligned} \tag{42}$$

Numerical requirements of using equation (41) are discussed in Wilson et al. [1991], where the marching procedure in equation (42) is shown to be unconditionally stable. As a result, the $O(h^2)$ notation is dropped hereafter. Over sufficiently small step-sizes, the integral from 0 to *h* can be approximated with a single-point expansion, which leaves the marching equation as

$$\begin{aligned}\phi_{sc}(z+h,E) = {} & e^{-\sigma(E)h}\phi_{sc}(z,E) \\ & +\sigma_0(E,E_L)e^{-\sigma(E_L)z}\,\frac{e^{-\sigma(E)h} - e^{-\sigma(E_L)h}}{\sigma(E_L)-\sigma(E)} \\ & +he^{-\sigma(E)h}\int_E^{E_L}\sigma_0(E,E')\phi_{sc}(z,E')dE'.\end{aligned} \tag{43}$$

Equation (43) is evaluated on a discrete energy grid with N_E points, allowing the integral to be approximately, but efficiently evaluated as

$$\begin{aligned}\phi_{sc}(z+h,E) &= e^{-\sigma(E)h}\phi_{sc}(z,E) \\ &+\sigma_0(E,E_L)e^{-\sigma(E_L)z}\,\frac{e^{-\sigma(E)h}-e^{-\sigma(E_L)h}}{\sigma(E_L)-\sigma(E)} \\ &+he^{-\sigma(E)h}\sum_{j=i}^{N_E-1}\big\langle\sigma\big\rangle_{ij}\big[\Phi_{sc}(z,E_j)-\Phi_{sc}(z,E_{j+1})\big],\end{aligned} \tag{44}$$

where

$$\big\langle\sigma\big\rangle_{ij} = \frac{1}{E_{j+1}-E_j}\int_{E_j}^{E_{j+1}}\sigma_0(E_i,E')dE', \tag{45}$$

$$\Phi_{sc}(z,E) = \int_E^{\infty}\phi_{sc}(z,E')dE'. \tag{46}$$

The solutions evaluated with the perturbative solution of equation (37) and the marching procedure of equation (44) are shown in Fig. 7 at four incident energies of E_L = 100, 200, 300, 400 MeV and various depths in nuclear matter. It is clear that the most important component is near the incident energy at small penetration depths but diminishes at higher order scattering where further degradation of energy dominates at the larger depths. It can also be seen that the two solution methodologies give nearly identical results, although the marching procedure is more computationally efficient.

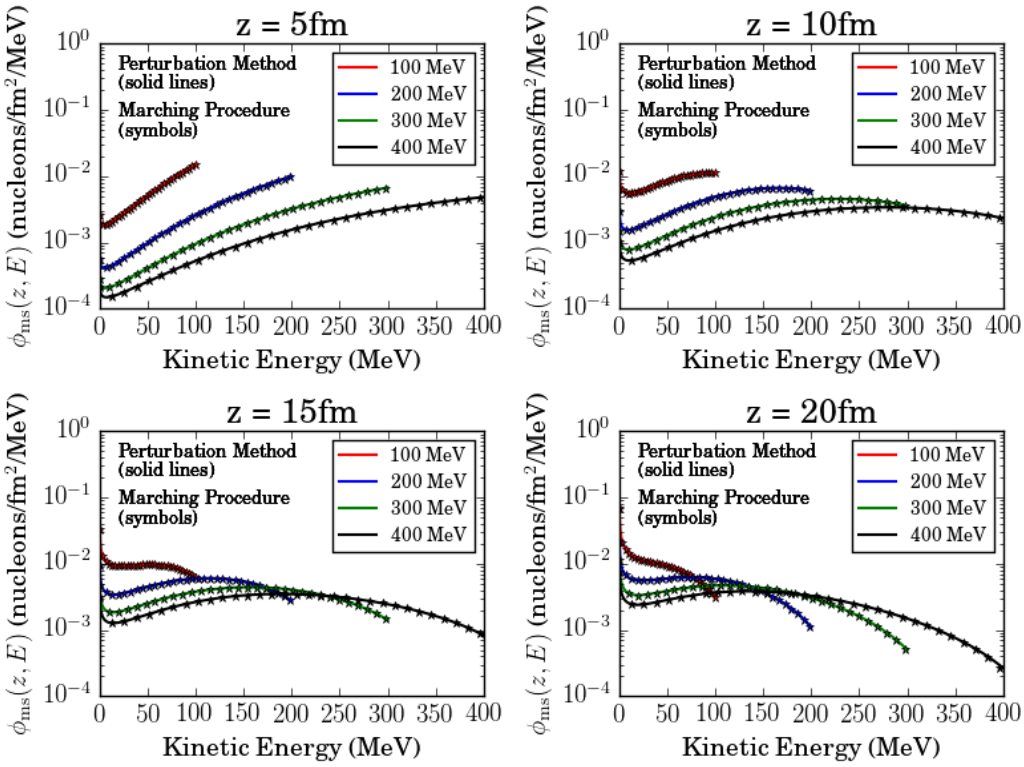

Fig. 7. Transmitted quasi-elastic spectra of a multiply scattered nucleon at four depths in nuclear matter as evaluated by equations (37) and (44) at four incident energies.

Connection to Ranft/Bertini Model in HZETRN

Following Wilson et al. [1986b], the transmitted fluence spectra of scattered nucleons (equivalently obtained with either the perturbative method or marching procedure) can be utilized to estimate the differential energy cross section of quasi-elastically produced nucleons. Such estimates can then be integrated into 3DHZETRN to replace the currently used parametric form given by equation (5). Minor modifications to the Ranft/Bertini nucleon production model currently used in 3DHZETRN are needed to complete the integration process and are described in this section.

Of particular importance is the evaluation of the absorption and the quasi-elastic cross sections for nucleons impacting target nuclei. Within the notation of Serber [1947], the absorption cross section (in units of fm^2) is related to attenuation of the scattered primary nucleon fluence incident on the target nucleus and given as

$$\sigma_{abs}(E_L) = 2\pi \int_0^\infty \left[1 - e^{-\sigma(E_L)\int_{-\infty}^{\infty} \rho(b,z)dz} \right] b\, db\,, \tag{47}$$

where ρ is the target nuclear density function evaluated from the charge densities [Wilson 1975, Wilson and Costner 1977, Wilson et al. 1991] normalized to unit density as accounted for by $\sigma(E_L)$ in units of fm^{-1}. An equivalent definition of the absorption cross section, utilizing the un-collided primary nucleon fluence ϕ_0(z,E), understood as the probability of suffering no collisions in penetration to depth *z*, is given as

$$\begin{aligned} \sigma_{abs}(E_L) &= 2\pi \int_0^\infty \; 1 - \int_0^\infty \phi_0[z(b), E]dE \;\; b\, db \\ &= 2\pi \int_0^\infty \left[1 - e^{-\sigma(E_L) z(b)} \right] b\, db \end{aligned} \tag{48}$$

where ϕ_0 was previously defined in equation (33), and *z*(*b*) is the penetration depth in a finite volume of nuclear matter for an impact parameter *b*. The absorption cross section defined in equation (47) or (48) includes both the reaction probability and average multiplicity and is consistent with the original definition for the absorption cross section given by the Serber model [1947].

Although equation (47) could be evaluated for any arbitrary density function, it will suffice herein to use a uniform sphere approximation allowing a simple evaluation as

$$\int_{-\infty}^{\infty} \rho(b,z)dz = 2\sqrt{R^2 - b^2} \equiv z(b)\,, \tag{49}$$

where $R = 1.29 a_A$ is the radius (fm) of the equivalent nuclear sphere [Wilson 1975], and the root mean square (RMS) radius, a_A, is found from the RMS charge radii given in Table 1 using $a_A = \sqrt{a_c^2 - 0.64}$. Note that the function *z*(*b*) defined in equation (49) gives the chord length through a nuclear sphere for an impact distance *b*.

Table 1. Root mean square nuclear charge radius, a_c (fm) [Hofstadter and Collard 1967].

A	a_c
1	0.84
2	2.17
3	1.78
4	1.63
$6 \le A \le 14$	2.40
$A \ge 16$	$0.58 + 0.82A^{1/3}$

Using equation (49), the absorption cross section is evaluated as

$$\sigma_{abs}(E_L) = 2\pi\int_0^R \Big[1 - e^{-2\sigma(E_L)\sqrt{R^2-b^2}}\Big] b\, db$$
$$= \pi R^2 + \frac{\pi \;\; e^{-2\sigma(E_L)R}\big[1 + 2\sigma(E_L)R\big] - 1}{2\big[\sigma(E_L)\big]^2} \;, \tag{50}$$

and the nucleon quasi-elastic differential cross section is found from

$$\tilde{\sigma}_{qe}(E, E_L) = 2\pi\int_0^R \phi_{ms}\big[z(b), E\big] b\, db \;, \tag{51}$$

where ϕ_{ms} is computed for an incident beam with energy E_L using either the perturbative method or marching procedure described in previous sections (marching procedure results are used hereafter for computational efficiency), and $z(b)$ is given by equation (49). Note that equation (51) is the nucleon quasi-elastic cross section; the specific isotopic (i.e. neutron or proton) components are not yet represented.

To make use of well-established nuclear reaction cross sections [Tripathi et al. 1997, 1998, 1999, 2002], the quasi-elastic differential cross section of equation (51) is re-normalized as

$$\sigma_{qe}(E, E_L) = \sigma_k(E_L)\frac{\tilde{\sigma}_{qe}(E, E_L)}{\pi R^2} \;, \tag{52}$$

where $\sigma_k(E_L)$ is the nuclear reaction cross section from Tripathi et al. [1997, 1998, 1999, 2002] for a type *k* projectile with kinetic energy E_L.

To preserve the isotopic distribution of the quasi-elastic cross section currently used in HZETRN, the fraction of type *j* particles (neutrons or protons) produced by collisions induced by type *k* projectiles (neutrons or protons) is evaluated as

$$f_{jk,qe}(E_L) = \frac{N_{jk,qe}(E_L)}{\sum_l N_{lk,qe}(E_L)}, \tag{53}$$

where $N_{jk,qe}(E_L)$ is the quasi-elastic multiplicity currently used in HZETRN obtained from the balance of Bertini multiplicities as described by Wilson et al. [1991]. The quasi-elastic cross section for this new model is given as

$$\sigma_{jk,qe}(E, E_L) = f_{jk,qe}(E_L)\sigma_{qe}(E, E_L) \,. \tag{54}$$

Note that in this new model, the ratio of quasi-elastically produced neutrons to protons remains the same as the current model in HZETRN [Wilson et al. 1991]; however, the overall magnitude and spectrum of the quasi-elastic component is determined by the new nuclear model.

A final element of integrating this new nuclear model into 3DHZETRN requires the quasi-elastic multiplicity to be efficiently evaluated such that it can be re-balanced against the Bertini cascade multiplicities as described in Wilson et al. [1991]. The total quasi-elastic multiplicity is given by

$$N_{jk,qe}(E) = f_{jk,qe}(E)\left[\frac{\sigma_{abs}(E)}{\pi R^2}\right], \tag{55}$$

where the term in brackets is the average number of primary nucleons transmitted through the target nuclear sphere.

If this simple extension of the Ranft/Bertini model currently used in HZETRN is successful, then a more complete description could be at hand by extending the formalism to treat isotopic components (with Pauli blocking) and other particle production processes, as had been started many years ago [Wilson et al. 1986b]. The next section demonstrates the impact of this new formalism on the *for*/*iso* assumption and the *qe/mp* model.

New Quasi-Elastic Model in HZETRN

The simple homogenous spherical geometry exposed to the Webber SPE considered in a prior section (see Fig. 4) is now re-evaluated with the new quasi-elastic cross section model. Using this new quasi-elastic cross section model in the *for*/*iso* and *qe*/*mp* transport formalisms of 3DHZETRN yields the results in Fig. 8. There are some encouraging improvements in the transport results with improved quasi-elastic cross sections in the 10 to few hundred MeV region. An expanded view of the prior quasi-elastic and the present quasi-elastic term is shown in Fig. 9 where it is clear that this re-evaluation has improved the comparisons with the MC codes. Future work will evaluate the multiple-production cross section effects on the current solutions and will include Pauli blocking, affecting both the quasi-elastic and multiple-production processes.

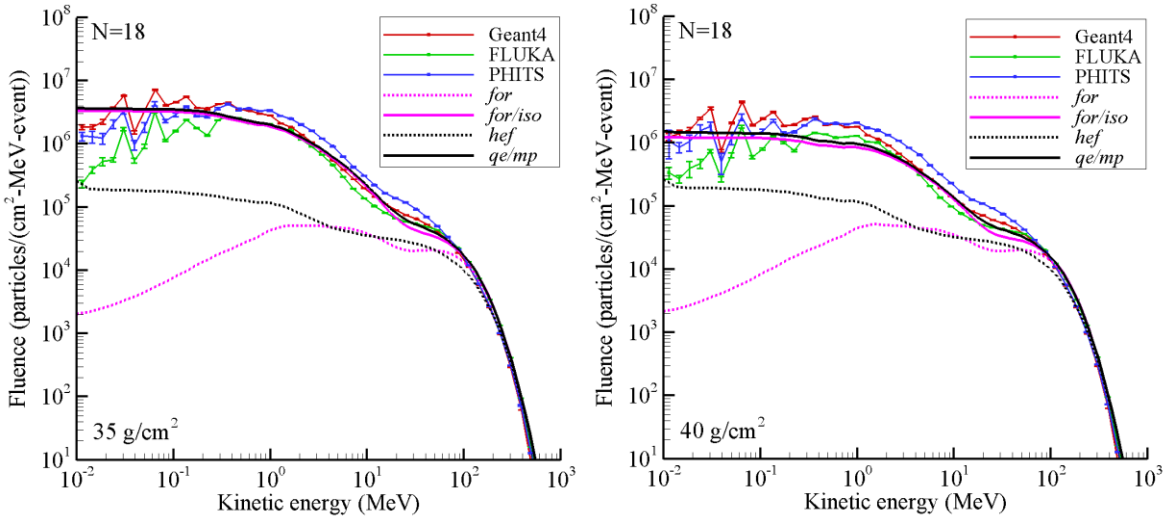

Fig. 8. Impact of current Serber model of quasi-elastic contribution to neutron fluence spectra in an aluminum sphere.

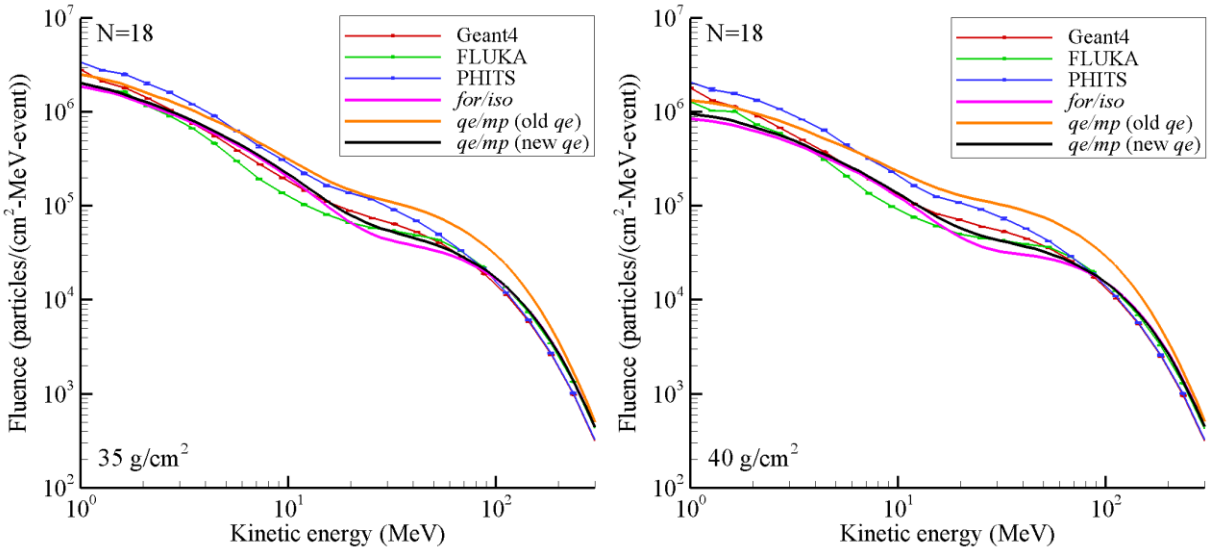

Fig. 9. Comparison of equation (3) quasi-elastic model with the new quasi-elastic model.

Conclusions

In this work the *for*/*iso* formalism in 3DHZETRN was replaced with a *qe*/*mp* formalism allowing angular dependence to be included in the multiple-production neutron source term. Using simplified spherical geometry exposed to the Webber SPE, it was found that the *qe*/*mp* transport formalism provides some improvement over the *for*/*iso* assumption. However, further improvements to the quasi-elastic component of the neutron production cross section are needed.

In order to improve the current quasi-elastic component, represented parametrically by equation (5), the Serber [1947] nuclear transport model was considered. Perturbative and numerical marching solutions were developed to solve the relevant equations representing transport of nucleons through a finite volume of nuclear matter. Details associated with nuclear binding were neglected. Methods for coupling the new quasi-elastic model into 3DHZETRN were also described.

The spherical geometry benchmark case was then re-evaluated using the new quasi-elastic cross section model, and it was found that modest improvements were achieved. Further work will focus on refining the implementation of the Serber model to include effects associated with nuclear binding and Pauli blocking.

Acknowledgements

This work was supported by the Human Research Program under the Human Exploration and Operations Mission Directorate of NASA and by NASA Grant number NNX09AR20A.

References

Agostinelli, S. et al., Geant4--a simulation toolkit. *Nucl. Instrum. & Methods A* **506**: 250-303; 2003.

Alsmiller, R.G., Irving, D.C., Kinney, W.E., Moran, H.S., The validity of the straight-ahead approximation in space vehicle shielding studies. In *Second Symposium on Protection Against Radiations in Space*, Arthur Reetz, ed. NASA SP-71, pp. 177-181, 1965.

Battistoni, G., Muraro, S., Sala, P.R., Cerutti, F., Ferrari, A., Roesler, S.,Fasso, A., Ranft, J., The FLUKA code: Description and benchmarking. *Proceedings of the Hadronic Shower Simulation Workshop 2006*, **896**: 31–49; 2007.

Chew, G.F., High energy elastic proton-deuteron scattering. *Phys. Rev.* **84**: 1057-1058; 1951.

Clowdsley, M.S., Heinbockel, J.H., Kaneko, H., Wilson, J.W., Singleterry, R.C., Shinn, J.L., A comparison of the multigroup and collocation methods for solving the low-energy neutron Boltzmann equation. *Can. J. Phys*. **78**: 45-56; 2000.

Clowdsley, M.S., Wilson, J.W., Shinn, J.L., Badavi, F.F., Heinbockel, J.H., Atwell, W., Neutron environment calculations for low Earth orbit. SAE 01ICES2327, 2001.

Cucinotta, F.A., Hajnal, F., Wilson, J.W., Energy deposition at the bone-tissue interface from nuclear fragments produced by high-energy nucleons. *Rad. Res.* **59**: 819-825; 1990.

Dymarz, R. and Kohmura, T., Determination of the nuclear interaction radius and transparency from the optical model phase shifts. *Phys. Lett. B* **117**: 145-149; 1982.

ENDF, Evaluated nuclear data file database; 2016. Available at https://www-nds.iaea.org/exfor/endf.htm.

Fasso, A., Ferrari, A., Ranft, J., Sala, P.R., FLUKA: A multi-particle transport code. CERN-2005-10, INFN/TC 05/11, SLAC-R-773, 2005.

Foelsche, T., Mendell, R.B., Wilson, J.W., Adams, R.R., Measured and calculated neutron spectra and dose equivalent rates at high altitudes: Relavance to SST operations and space research. NASA TN D-7715, 1974.

Goldberger, M.L., The interaction of high energy neutrons and heavy nuclei. *Phys. Rev.* **74**: 1269-1277; 1948.

Heinbockel, J.H., Feldman, G.A., Wilson, J.W., Singleterry, R.C., Leakeas, C.L., Clowdsley, M.S., Solutions to the low energy neutron Boltzmann equation for space applications. SAE 03ICES339, 2003.

Heinbockel, J.H., Slaba, T.C., Blattnig, S.R., Tripathi, R.K., Townsend, L.W., Handler, T., Gabriel, T.A., Pinsky, L.S., Reddell, B., Clowdsley, M.S., Singleterry, R.C., Norbury, J.W., Badavi, F.F., Aghara, S.K., Comparison of the transport codes HZETRN, HETC and FLUKA for a solar particle event. *Adv. Space Res.* **47:** 1079-1088; 2011.

Hofstadter, R. and Collard, H.R., *Nuclear Radii Determination by Electron Scattering,* Landolt-Börnstein Series, Vol. 2, Springer-Verlag, Berlin-Heidelberg-New York, 1967.

Lamkin, S.L., A theory for high-energy nucleon transport in one-dimension. Masters Thesis, Old Dominion University, June 1974.

Matthia, D., Ehresmann, B., Lohf, H., Kohler, J., Zeitlin, C., Appel, J., Sato, T., Slaba, T.C., Martin, C., Berger, T., Boehm, E., Boettcher, S., Brinza, D.E., Burmeister, S., Guo, J., Hassler, D.M., Posner, A., Rafkin, S.C.R., Reitz, G., Wilson, J.W., Wimmer-Schweingruber, R.F., The Martian surface radiation environment – a comparison of models and MSL/RAD measurements. *J. Space Weather* **6**: A13; 2016.

Ranft, J., The FLUKA and KASPRO hadronic cascade codes. *Computer Techniques in Radiation Transport and Dosimetry,* W. R. Nelson and T.M. Jenkins, eds, Plenum Press, pp. 339-371, 1980

Sato, T., Niita, K., Matsuda, N., Hashimoto, S., Iwamoto, Y., Noda, S., Ogawa, T., Iwase, H.,Nakashima, H., Fukahori, T., Okumura, K., Kai, T., Chiba, S., Furuta T., Sihver, L., Particle and heavy ion transport code system PHITS, version 2.52. *J. Nucl. Sci. Technol.* **50**: 913-923; 2013.

Serber, R., Nuclear reactions at high energies. *Phys. Rev*. **72**: 1114-1115; 1947.

Shavers, M.R., Poston, J.W., Cucinotta, F.A., Wilson, J.W., Biological effectiveness of nuclear fragments produced by high-energy protons interacting in tissues near the bone-soft tissue interface. *Health Phys.* **70**: 473-483; 1996.

Slaba, T.C., Blattnig, S.R., Badavi, F.F., Faster and more accurate transport procedures for HZETRN. *J. Comp. Phys.* **229**: 9397-9417; 2010a.

Slaba, T.C., Blattnig, S.R., Aghara, S.K., Townsend, L.W., Handler, T., Gabriel, T.A., Pinsky, L.S., Reddell, B., Coupled neutron transport for HZETRN. *Radiat. Meas.* **45**: 173-182; 2010b.

Slaba, T.C., Blattnig, S.R., Reddell, B., Bahadori, A., Norman, R.B., Badavi, F.F., Pion and electromagnetic contribution to dose: Comparisons of HZETRN to Monte Carlo results and ISS data. *Adv. Space Res.* **52**: 62-78; 2013.

Slaba, T.C., Wilson, J.W., Badavi, F.F., Redell, B.D., Bahadori, A.A., Solar proton exposure of an ICRU sphere within a complex structure part II: ray-trace geometry. *Life Sci. Space Res.* **9**: 77–83; 2016.

Tripathi, R.K., Cucinotta, F.A., Wilson, J.W., Universal parameterization of absorption cross sections. NASA TP 3621, 1997.

Tripathi, R.K., Wilson, J.W., Cucinotta, F.A., Nuclear absorption cross sections using medium modified nucleon-nucleon amplitudes. *Nucl. Instrum. & Methods B* **145**: 277-282; 1998.

Tripathi, R.K., Cucinotta, F.A., Wilson, J.W., Universal parameterization of absorption cross sections – light systems. NASA TP 1999-209726, 1999.

Tripathi, R.K., Wilson, J.W., Cucinotta, F.A., A method for calculating proton-nucleus elastic cross-sections. *Nucl. Instrum. & Methods B* **194**: 229-36; 2002.

Webber, W.R., An evaluation of solar-cosmic-ray events during solar minimum. D2-84274-1, Boeing Co. 1966.

Wilson, J.W., Intermediate energy nucleon-deuteron elastic scattering. *Nuc. Phys. B* **66**: 221-244; 1973.

Wilson, J.W., Multiple scattering of heavy ions, Glauber theory, and optical model. *Phys. Lett. B* **52**: 149-152; 1974.

Wilson, J.W. and Khandelwal, G.S., Proton dose approximation in convex geometry. *Nucl. Tech*. **23**: 298-305; 1974.

Wilson, J.W. and Lamkin, S.L., Perturbation approximation to charged particle transport. *Trans. Am. Soc*., **19**: 443; 1974.

Wilson, J.W., *Composite Particle Reaction Theory*, Ph.D. Dissertation, College of William and Mary, Williamsburg, Virginia, 1975.

Wilson, J.W. and Lamkin, S.L, Perturbation theory for charged-particle transport in one dimension. *Nucl. Sci. & Eng.* **57**: 292-299; 1975.

Wilson, J.W., Analysis of the theory of high-energy ion transport. NASA TN D-8381, 1977.

Wilson, J.W. and Costner, C.M. Nucleon and heavy ion total and absorption cross sections for selected nuclei. NASA TN D-8107, 1977.

Wilson, J.W. and Badavi, F.F., Methods of galactic heavy ion transport. *Rad. Res*. **108**: 231-237; 1986a.

Wilson, J.W., Townsend, L.W., Cucinotta, F.A., Transport model of nucleon-nucleus section. NASA TM 87724, 1986b.

Wilson, J.W., Townsend, L.W., Badavi, F.F., Galactic cosmic ray propagation in earth's atmosphere. *Radiat. Res.* **109**: 173-183; 1987a.

Wilson, J.W., Townsend, L.W., Badavi, F.F., A semiempirical nuclear fragmentation model. *Nucl. Instrum. & Methods B* **18**: 225-231; 1987b.

Wilson, J.W., Townsend, L.W., Chun, S.Y., Buck, W.W., Khan, F., Cucinotta, F.A., BRYNTRN: a baryon transport computer code, computational procedures and data base. NASA TM 4037, 1988a.

Wilson, J.W., Chun, S. Y., Buck, W.W., Townsend, L.W., High energy nucleon data bases. *Health Phys*. **55**: 817-819; 1988b.

Wilson, J.W., Townsend, L.W., Schimmerling, W., Khandelwal, G.S., Khan, F., Nealy, J.E., Cucinotta, F.A., Simonsen, L.C., Shinn, J.L., Norbury, J.W., Transport methods and interactions for space radiations. NASA RP 1257; 1991.

Wilson, J.W., Townsend, L.W., Shinn, J.L., Badavi, F.F., Lamkin, S.L., Galactic cosmic ray transport methods: past, present, and future. *Adv. Space Res*. **14**: 841-852; 1994.

Wilson, J.W., Tripathi, R. K., Cucinotta , F. A., Shinn, J. L., Badavi, F. F., Chun, S. Y., Norbury, J. W., Zeitlin, C. J., Heilbronn, L. H., Miller, J., NUCFRG2, an evaluation of the semiempirical nuclear fragmentation database. NASA TP-3533, 1995.

Wilson, J.W., Cucinotta, F.A., Tai, H., Shinn, J.L., Chun, S.Y., Tripathi, R.K., Sihver, L., Transport of light ions in matter. *Adv. Space Res.* **21**: 1763-1771; 1998.

Wilson, J.W., Tripathi, R.K., Mertens, C.J., Blattnig, S.R., Clowdsley, M.S., Verification and validation: High charge and energy (HZE) transport codes and future development. NASA TP 2005-213784, 2005.

Wilson, J.W., Tripathi, R.K., Badavi, F.F., Cucinotta, F.A., Standardized radiation shield design method: 2005 HZETRN. SAE/ICES paper 2006-01-2109, 2006.

Wilson, J.W., Nealy, J.E., Dachev, Ts.P., Tomov, B.T., Cucinotta, F.A., Badavi, F.F., De Angelis, G., Atwell, W., Leutke, N., Time serial analysis of the induced LEO environment within the ISS 6A. *Adv. Space Res.* **40**: 1562-1570; 2007.

Wilson, J.W., Slaba, T.C., Badavi, F.F., Reddell, B.D., Bahadori, A.A., A 3DHZETRN code in a spherical uniform sphere with Monte Carlo verification. NASA TP 2014-218271, 2014a.

Wilson, J.W., Slaba, T.C., Badavi, F.F., Reddell, B.D., Bahadori, A.A., Advances in NASA radiation transport research: 3DHZETRN. *Life Sci. Space Res.* **2**: 6-22; 2014b.

Wilson, J.W., Slaba, T.C., Badavi, F.F., Reddell, B.D., Bahadori, A.A., 3D space radiation transport in a shielded ICRU tissue sphere. NASA TP 2014-218530, 2014c.

Wilson, J.W., Slaba, T.C., Badavi, F.F., Reddell, B.D., Bahadori, A.A., 3DHZETRN: shielded ICRU spherical phantom. *Life Sci. Space Res.* **4**: 46-61; 2015a.

Wilson, J.W., Slaba, T.C., Badavi, F.F., Reddell, B.D., Bahadori, A.A., A study of neutron leakage in finite objects. NASA TP 2015-218692, 2015b.

Wilson, J.W., Slaba, T.C., Badavi, F.F., Reddell, B.D., Bahadori, A.A., 3DHZETRN: neutron leakage in finite objects. *Life Sci. Space Res.* **7**: 27-38; 2015c.

REPORT DOCUMENTATION PAGE

Form Approved
OMB No. 0704-0188

1. REPORT DATE *(DD-MM-YYYY)*	2. REPORT TYPE	3. DATES COVERED *(From - To)*
01- 03 - 2017	Technical Publication	

4. TITLE AND SUBTITLE

Neutron Angular Scatter Effects in 3DHZETRN: Quasi-Elastic

5a. CONTRACT NUMBER

5b. GRANT NUMBER

5c. PROGRAM ELEMENT NUMBER

6. AUTHOR(S)

Wilson, John W.; Werneth, Charles M.; Slaba, Tony C.; Badavi, Francis F.; Reddell, Brandon D.; Bahadori, Amir A.

5d. PROJECT NUMBER

5e. TASK NUMBER

5f. WORK UNIT NUMBER

651549.02.07.10

7. PERFORMING ORGANIZATION NAME(S) AND ADDRESS(ES)

NASA Langley Research Center
Hampton, VA 23681-2199

8. PERFORMING ORGANIZATION REPORT NUMBER

L-20794

9. SPONSORING/MONITORING AGENCY NAME(S) AND ADDRESS(ES)

National Aeronautics and Space Administration
Washington, DC 20546-0001

10. SPONSOR/MONITOR'S ACRONYM(S)

NASA

11. SPONSOR/MONITOR'S REPORT NUMBER(S)

NASA-TP-2017-219597

12. DISTRIBUTION/AVAILABILITY STATEMENT

Unclassified - Unlimited
Subject Category 93
Availability: NASA STI Program (757) 864-9658

13. SUPPLEMENTARY NOTES

14. ABSTRACT

The current 3DHZETRN code has a detailed three dimensional (3D) treatment of neutron transport based on a forward/isotropic assumption and has been compared to Monte Carlo (MC) simulation codes in various geometries. In most cases, it has been found that 3DHZETRN agrees with the MC codes to the extent they agree with each other. However, a recent study of neutron leakage from finite geometries revealed that further improvements to the 3DHZETRN formalism are needed. In the present report, angular scattering corrections to the neutron fluence are provided in an attempt to improve fluence estimates from a uniform sphere. It is found that further developments in the nuclear production models are required to fully evaluate the impact of transport model updates. A model for the quasi-elastic neutron production spectra is therefore developed and implemented into 3DHZETRN.

15. SUBJECT TERMS

HZETRN; Radiation; Space exploration; Transport

16. SECURITY CLASSIFICATION OF:			17. LIMITATION OF ABSTRACT	18. NUMBER OF PAGES	19a. NAME OF RESPONSIBLE PERSON
a. REPORT	b. ABSTRACT	c. THIS PAGE			STI Help Desk (email: help@sti.nasa.gov)
U	U	U	UU	29	19b. TELEPHONE NUMBER *(Include area code)* (757) 864-9658